NJC

ROYAL SOCIETY OF CHEMISTRY

PAPER

View Article Online
View Journal | View Issue

Check for updates

Cite this: *New J. Chem.*, 2021, **45**, 8335

Sustainable synthesis of 1,8-dioxooctahydroxanthenes in deep eutectic solvents (DESs)†

M. Shaibuna,[a] Anshad Abbas,[b] Muhammed Jeneesh Kariyottu Kuniyil[c] and K. Sreekumar *[a]

Received 12th February 2021,
Accepted 31st March 2021

DOI: 10.1039/d1nj00743b

rsc.li/njc

Deep eutectic solvents are obtained by the fusion of two or more compounds: hydrogen bond donors (HBDs) and hydrogen bond acceptors (HBAs). They are formed by mixing the constituents with moderate heating (*via* hydrogen bond interactions). In this manuscript, the dual activities (as catalysts and reaction media) of six deep eutectic solvents were compared for the synthesis of 1,8-dioxooctahydroxanthenes at room temperature. Here DES 2, a combination of $ZrOCl_2{\cdot}8H_2O$ with ethylene glycol at a 1 : 2 ratio, was found to be the supreme catalyst among the six DESs and was reused for five batches. The photophysical properties of the xanthene derivatives were examined by UV-vis and fluorescence spectroscopy in THF. The synthesised molecules showed absorption maxima around 285–295 nm and emission maxima around 403–404 nm. The ground state dipole moments of all the molecules were calculated by the Debye–Guggenheim method using toluene as the non-polar solvent. All the synthesised molecules showed significant dipole moment values and are in good agreement with theoretical values.

Introduction

Global warming issues are raising more concerns in favour of introducing new green methods in chemistry. One among them is use of deep eutectic solvents (DESs), a new generation of solvents, first introduced by Abbott *et al.*[1] The main highlights of DESs are their low toxicity, low cost, biodegradability, biocompatibility, reusability, mild preparation methods, non-flammability, non-volatility, *etc.*[2] DESs are also called designer solvents or tailormade solvents because their properties can be designed by changing the constituents used and are good alternatives to traditional organic solvents.[3] The influences of strong hydrogen bond donors (HBDs) on the physical properties, like density, viscosity, acidity, and conductivity, of DESs are reported and are very significant in tailoring DESs for specific purposes.[4] In addition to this, the variations of physico-chemical properties, like density, viscosity, conductivity, and surface tension, with temperature were studied in previous reports.[4,5] Most recent publications encompass the application of DESs in distinct fields, like CO_2 capture technology,[6] liquid–liquid extraction,[7] photophysical behavior and fluorescence quenching studies,[8] as media for valorization of monosaccharides towards fructopyrazines,[9] atom transfer radical polymerisation (ATRP),[10] in concentrated solar power (CSP) plants,[11] biomass pretreatment and conversion,[12] chromatography,[13] extraction of isoflavones from chickpeas[14] and quercetin from vegetables,[15] extraction of wheat straw to produce lignin nanoparticles,[16] *etc.* Recently, acidic deep eutectic solvents formed from *p*-toluenesulfonic acid (*p*-TsOH) and quaternary ammonium salts with different carbon chains were used as catalysts as well as reaction media for biodiesel production from cooked and waste vegetable oil.[17] Catalysis is the most important application of DESs to overcome the shortcomings of conventional organic solvents and costly catalysts. Many recent publications highlight their activity in organic synthesis; these include cycloaddition of CO_2 with propylene oxide,[18] glycolysis of polyethylene terephthalate,[19] amidation reaction,[20] the oxygen evolution reaction,[21] esterification reaction, *etc.*[4,5]

Due to the wide applicability of heterocyclic compounds, their synthesis have attracted widespread attention in synthetic and medicinal chemistry. Especially, such compounds with xanthene ring systems display many pharmacological properties such as antitumour,[22] antibacterial and antifungal,[23] anticonvulsant,[24] antiplasmodial,[25] antinociceptive,[26]antiinflammatory,[27] photodynamic therapeutic[28] and DNA binding[29] properties.

---

[a] *Department of Applied Chemistry, Cochin University of Science and Technology, Cochin-22, India. E-mail: kskpolymer.cusat@gmail.com*
[b] *Department of Physics, Cochin University of Science and Technology, Cochin-22, India*
[c] *Department of Chemistry, Pondicherry University, R V Nagar, Kalapet, Puducherry 605 014, India*

† Electronic supplementary information (ESI) available. See DOI: 10.1039/d1nj00743b

Also they are used as antagonists for the paralyzing action of zoxazolamine[30] and drug-resistant leukemia lines.[31] In addition, they are used as fluorescent materials (pH sensitive) for visualization of biomolecules,[32] local-dyes,[33] laser technologies,[34] cosmetics and pigments,[35] novel CCR1 receptor antagonists,[36] and inhibitors of recombinant human calpain I.[37] Besides all these, they are considered as important synthons because of the inherent reactivity of the inbuilt pyran ring.[38] Common methods for the synthesis of 9-aryl-1,8-dioxooctahydroxanthenes involve the reaction of aldehydes with dimedone in a 1 : 2 ratio. Conventionally used catalysts for the synthesis of 9-aryl-1,8-dioxooctahydroxanthenes include protonic acids,[39] acidic clays,[40] catalysts based on silica,[41] Lewis acids,[42] ionic liquids,[43] *etc.* Furthermore, many new catalysts were also introduced in recent times, like sulfonamide functionalized magnetic composites,[44] nickel-cobalt ferrite NPs,[45] carbon-based nanocatalysts,[46] $CuFe_2O_4@SiO_2@C_3$-Imid-C_4SO_3-PW magnetic nanoparticles,[47] cobalt nanoparticles,[48] nickel NPs@N-doped titania nanocatalysts,[49] and caffeine-based ionic liquids.[50] Most of them are nanoparticles, which require multistep preparation processes and also harsh reaction conditions, prolonged reaction times, appropriate experimental setups, higher temperatures, the presence of organic solvents, costly catalysts, the formation of by-products, *etc.* All the above mentioned obstacles emphasize the requirement of new green methods, which can completely overcome the problems associated with this.

In this context, the introduction of deep eutectic solvents (DESs) acquires significance; they can act as catalysts as well as reaction media, and their easy method of preparation is the main highlight here (formed by mixing the components with gentle heating at different ratios, and the DESs are obtained with 100% atom economy). In this work, a comparative study was performed based on the catalytic activities of six DESs for the synthesis of 1,8-dioxooctahydroxanthenes. The absorption and emission spectra of the products were recorded in THF. Dipole moment measurement was carried out to explore the applicability of xanthene derivatives in areas like electrooptic devices and photorefractive materials. The basic requirements for such applications are asymmetric charge distribution and polarisability.[51] For that, the ground state dipole moment was experimentally determined by the Debye–Guggenheim method using toluene as solvent. High dipole moment values were obtained, which indicated the unsymmetrical electronic structures, stronger intermolecular interactions and polarization of the molecules. Attempts were made to calculate the excited state dipole moment by monitoring the solvatochromic behaviour assuming a two-level model. But the molecules did not show significant solvatochromism, so experiments for excited state dipole moment studies were not conducted. In order to verify the dipole moment obtained from the experiment and to find whether the yields of the xanthene derivatives depended on the ground state energy of the molecules, the molecules were optimized using the DFT/B3LYP/6-31G* formalism by employing Gaussian 09.[52]

Results and discussion

Six deep eutectic solvents formed from $ZrOCl_2{\cdot}8H_2O/CeCl_3{\cdot}7H_2O$ in combination with urea/ethylene glycol/glycerol were reported along with the study of their physicochemical properties and have been successfully applied as catalysts and solvents for the Paal–Knorr pyrrole synthesis,[53] Knoevenagel condensation reaction[54] and Kabachnik–Fields reaction.[55] The catalysts prepared with their corresponding ratios are given in Table 1. In order to check further the applicability of the catalysts in organic synthesis, the reaction between benzaldehyde and dimedone was selected as a model reaction for the synthesis of xanthene derivatives. At first, the reaction was conducted between benzaldehyde (1 mmol) and dimedone (2 mmol) in the absence of a catalyst and solvent at room temperature. The Knoevenagel product was observed instead of a xanthene derivative even after 24 h. This indicated the necessity of a catalyst in this reaction. Later the same reaction was repeated using 1 mmol of different catalysts (DES 1–DES 6) at room temperature. A mixture of the Knoevenagel product and 1,8-dioxooctahydroxanthene (with GC yields of 16.945% and 83.056%, respectively) was observed in DES 1 (Table 1, entry 1) and their corresponding gas chromatograms and mass spectra are given in Fig. 1.

The expected 1,8-dioxooctahydroxanthene was formed in the presence of DES 2 in good to excellent yield without any side product (Table 1, entry 2), and a low yield was observed in DES 3. The variation in activity of DESs may be due to the difference in hydrogen bonding ability of the DESs during the reaction. DES 1 is the most acidic catalyst (pH = 2.20) among the six DESs,[53,54] but it could not completely convert the reactants into products, and an intermediate Knoevenagel product (derivative of 1,3-diketone) was present in good quantity in addition to 1,8-dioxooctahydroxanthenes (the amounts of xanthene and Knoevenagel product were 83.056% and 16.945%, respectively, Table 1, entry 1). Such a trend was not observed in the case of DES 2. The intermediate (Knoevenagel product) was completely converted into the desired product even though DES 2 was not acidic in the conventional sense (pH = 6.99) compared to the

Table 1 Prepared DESs with their catalytic activity

Entry	DES	Molar ratio	Abbreviation	pH	Viscosity (η)/(mPa s)	Product formed
1	Zr : U	1 : 5	DES 1	2.20	52.40	Mixture of products
2	Zr : EG	1 : 2	DES 2	6.93	149.50	Xanthene derivative (96%)
3	Zr : Gly	1 : 2	DES 3	6.97	532.73	Xanthene derivative (65%)
4	Ce : U	1 : 5	DES 4	4.71	195.39	Knoevenagel product (97%)
5	Ce : EG	1 : 2	DES 5	4.44	290.40	Xanthene derivative (55%)
6	Ce : Gly	1 : 2	DES 6	4.27	868.73	Xanthene derivative (40%)

Zr = $ZrOCl_2{\cdot}8H_2O$, Ce = $CeCl_3{\cdot}7H_2O$, U = urea, EG = ethylene glycol, Gly = glycerol. Reaction conditions: benzaldehyde (1 mmol), dimedone (2 mmol) and DES 2 (1 mmol), 30 min, RT.

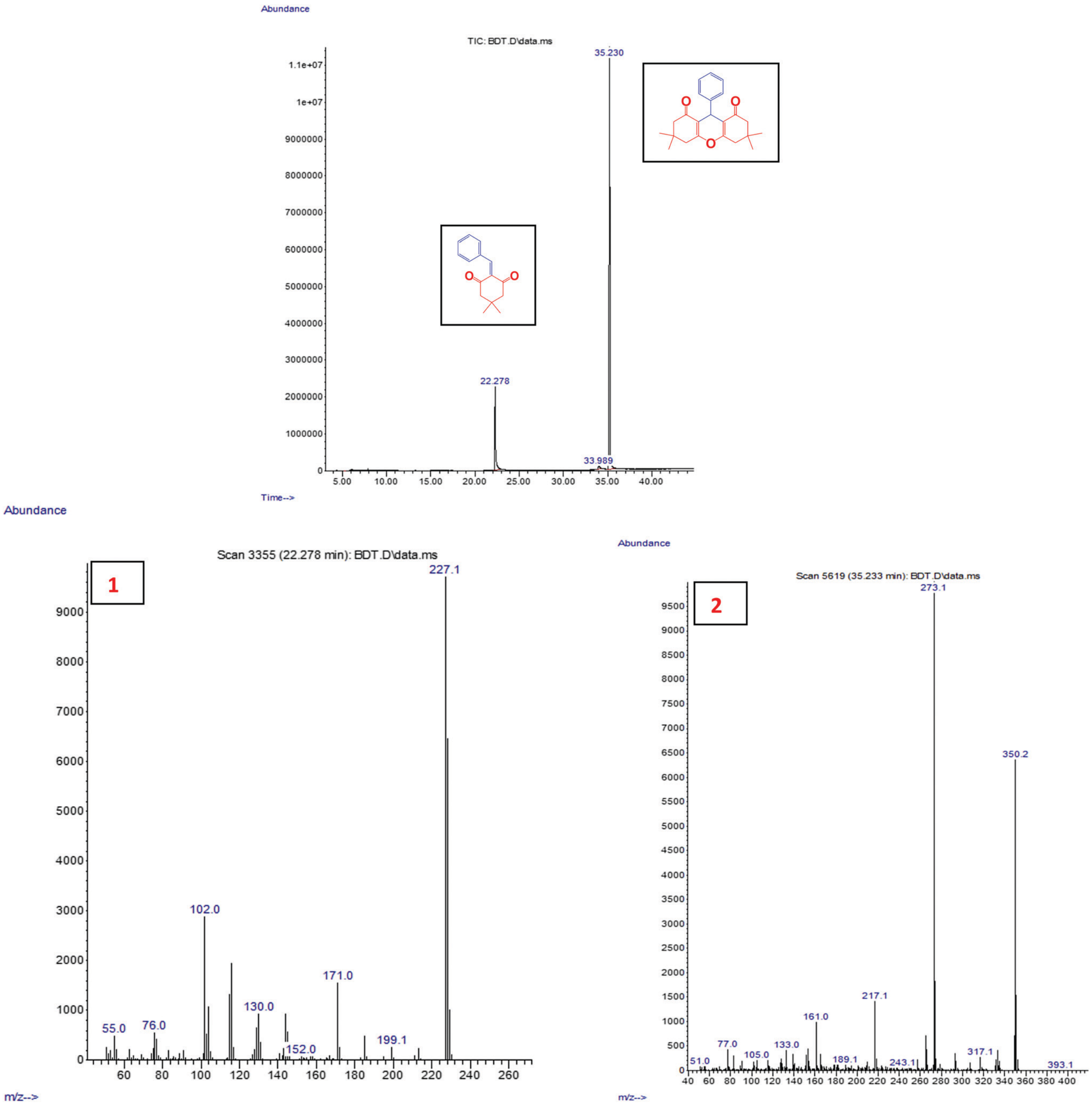

Fig. 1 Gas chromatograms and mass spectra of the corresponding Knoevenagel product (1) and xanthene derivative (2).

remaining DESs like DES 1 (pH = 2.20), DES 4 (pH = 4.71), DES 5 (pH = 4.44) and DES 6 (pH = 4.27). Only xanthene derivatives were formed even at a 1 : 1 ratio of benzaldehyde and dimedone using DES 2; this explained the activity of DES 2, which was based on the hydrogen bonding ability of the catalysts, not their acidity. A low yield was observed in the case of DES 3 (formed from $ZrOCl_2 \cdot 8H_2O$ and glycerol at a 1 : 2 ratio), which may be due to the higher viscosity of DES 3 (532.73 mPa s), which may prevent the free motion of the reactants during the reaction and prevent the reactivity.[55] Similarly, the catalytic activities of DES 4–DES 6 were unsatisfactory. Only the Knoevenagel product was observed in DES 4 (Table 1, entry 4) and xanthene derivatives with lower yields were observed in DES 5 and DES 6 (Table 1, entries 5 and 6).

This indicates that acidity is not the most important factor in determining the catalytic activity in the present reaction. The excellent catalytic activity of DES 2 may be due to its strong ability to activate the aldehyde through hydrogen bonding interaction. In addition to this, the lower viscosity of DES 2 (149.50 mPa s, Table 1, entry 2) may also favour the reaction by allowing the free motion of the reactants during the reaction and makes the reaction faster. Here, DES 2 perform dual roles

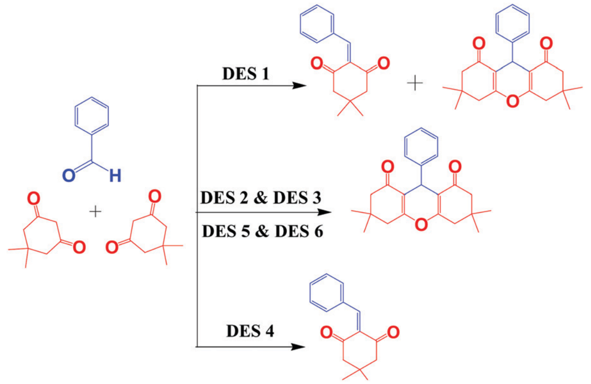

Scheme 1 Reaction of benzaldehyde with dimedone (1 : 2 ratio) in DES 1–DES 6.

as catalysts and reaction medium; the catalytic activity may be favoured by the strong hydrogen bonding ability of DES 2 and the solvent activity was favoured by its lower viscosity. This simultaneous effect contributed to the better activity of DES 2 for the synthesis of 1,8-dioxooctahydroxanthenes. The scheme of the reaction is given in Scheme 1. The excellent catalytic activity of DES 2 was previously reported for the synthesis of symmetric dihydropyridines from aldehydes, ethyl acetoacetate and ammonium acetate.[56]

The reaction was repeated using some other aldehydes in the presence of the six DESs under the same conditions to confirm the activity of the catalysts and the purity of products. All the products were formed with excellent purity and there was no side product like 2,2′-arylmethylene bis(3-hydroxy-5,5-dimethyl-2-cyclohexene-1-one) (an open chain form of xanthene derivative), which is a major problem in some previous methods. They are formed through the Knoevenagel/Michael reaction without undergoing a cyclodehydration step. Normally, 1,8-dioxooctahydroxanthenes are formed *via* the Knoevenagel/Michael/cyclodehydration reaction (Scheme 2). From this, it was concluded that DES 2 was the better catalyst among the six DESs for the synthesis of 1,8-dioxooctahydroxanthene derivatives.

Based on these findings, the reaction was repeated using different amounts of catalysts and the time required for the completion was noted using TLC analysis; the results are given in Table 2. At first, the reaction was carried out using benzaldehyde and dimedone as model substrates in the presence of 0.1 mmol of DES 2 at room temperature; it took 1 hour to complete the reaction with 60% yield. The reaction was repeated using different amounts of DES 2 with the same substrates (Table 2, entries 2–8); an outstanding yield was obtained using 0.5 mmol of DES 2 and this is the optimum catalyst amount needed for the reaction. In order to determine the optimum time required for the reaction, the reaction was repeated using this optimum catalyst amount and completion of the reaction was monitored using TLC. The observations are given in Table 2 (entries 9–12). An excellent yield was obtained within 15 minutes (Table 2, entries 11 and 12) and this is the optimum time needed for the reaction.

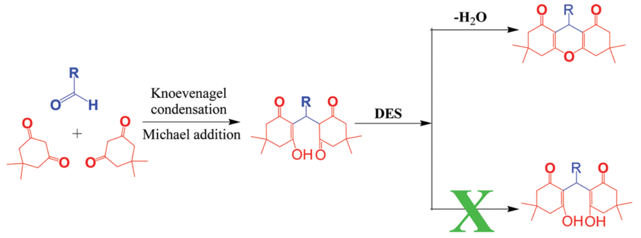

Scheme 2 Formation of 1,8-dioxooctahydroxanthenes and their open chain forms.

Table 2 Optimisation of catalyst amount and time

	Catalyst			
Entry	(g)	(mmol)	Time	Yield (%)
1	—	—	24 h	No reaction
2	0.0446	0.1	1 h	60
3	0.0892	0.2	1 h	64
4	0.1338	0.3	1 h	72
5	0.1784	0.4	1 h	80
6	0.2230	0.5	1 h	96
7	0.2676	0.6	1 h	97
8	0.3122	0.7	1 h	96
9	0.2230	0.5	30 min	96
10	0.2230	0.5	20 min	95
11	0.2230	0.5	15 min	96
12	0.2230	0.5	10 min	80

Reaction conditions: benzaldehyde (1 mmol), dimedone (2 mmol), DES 2, RT.

Table 3 Substrate scope of the reaction

Entry	R	Product	Time (min)	Yield (%)
1	H	X1	15	96
2	2-OH	X2	15	92
3	4-OH	X3	20	93
4	2-OMe	X4	25	96
5	4-OMe	X5	25	88
6	4-Cl	X6	20	89
7	4-Br	X7	15	85
8	4-NO$_2$	X8	20	90
9	1-Furyl	X9	30	Lower yield
10	1-Thienyl	X10	10	90
11	Cinnamyl	X11	30	88

Reaction conditions: aldehydes (1 mmol), dimedone (2 mmol), DES 2 (0.5 mmol), RT.

With these optimised conditions in hand, the reaction was repeated using different aldehydes; the corresponding time and yield were noted and are given in Table 3 (entries 1–11). Both electron withdrawing and donating groups on the aromatic aldehyde reacted efficiently with excellent yields (ranging between 85 and 96% with time periods of 15–30 min). The reaction was repeated using heteroaromatic aldehydes like thiophenaldehyde and furfural; an excellent yield and purity

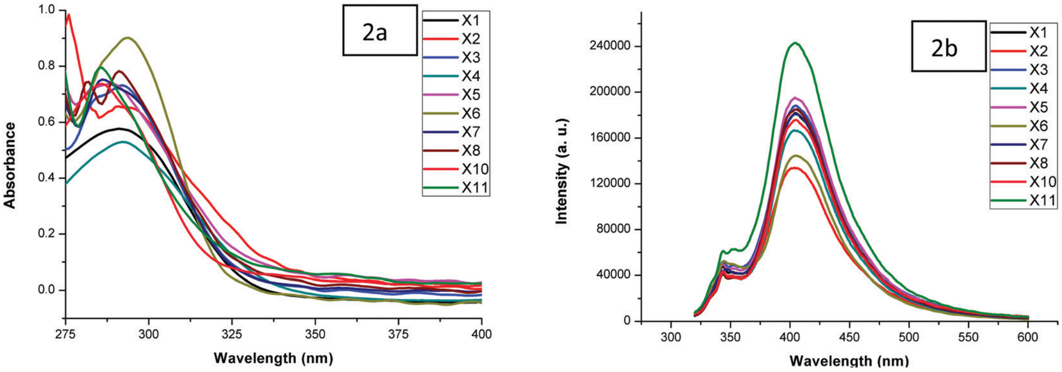

Fig. 2 (a) UV–vis absorption spectra and (b) emission spectra of products in THF.

were observed in the case of thiophenaldehyde, but a low yield with impurity was observed in the case of furfural (there was no improvement observed upon the addition of catalyst or variation of reaction time), which may be due to the polymerisable nature of the furyl ring. Similarly, efficient conversion was observed for an unsaturated aldehyde (cinnamaldehyde). After completion of the reaction, the recyclability was checked and the DES was reused up to 5 runs without any noticeable loss in catalytic activity.

Table 4 UV-vis and fluorescence spectral data of the xanthene derivatives

Entry	R	Compound	Absorption λ_{max} (nm)	Emission λ_{max} (nm)
1	H	X1	291	404
2	2-OH	X2	293	403
3	4-OH	X3	291	404
4	2-OMe	X4	292	403
5	4-OMe	X5	288	404
6	4-Cl	X6	293	404
7	4-Br	X7	286	403
8	4-NO_2	X8	291	404
9	1-Furyl	X9	—	—
10	1-Thienyl	X10	285	403
11	Cinnamyl	X11	286	403

Due to the extended conjugation of xanthenedione with an inbuilt pyran ring, xanthene derivatives are supposed to exhibit optical behavior. Here, after completion of the synthesis of 1,8-dioxooctahydroxanthenes, the absorption and fluorescence spectra of all the molecules except for the product corresponding to furfural (lower yield with impurity) were recorded in THF (excitation wavelength = 300 nm). The spectra are shown in Fig. 2a and b.

Here, the synthesised molecules showed absorption maxima around 285–295 nm and emission maxima of all the molecules were around 403–404 nm. The synthesised molecules showed similar absorption maxima (around 285–295 nm) and emission maxima (around 403–404 nm) and there was no difference in the values for either electron-donating or electron-withdrawing groups. The products with their corresponding absorption and emission maxima [λ_{max} (nm)] are given in Table 4.

Determination of ground state dipole moments (μ_g)

The dipole moment is an indication of polarity in a molecule. Here, the ground state dipole moments of the molecules were calculated by the Debye–Guggenheim method using toluene as the non-polar solvent.[46] To calculate the dielectric constant, several concentrations of the molecules except for the product corresponding to furfural (X9-lower yield with impurity) in

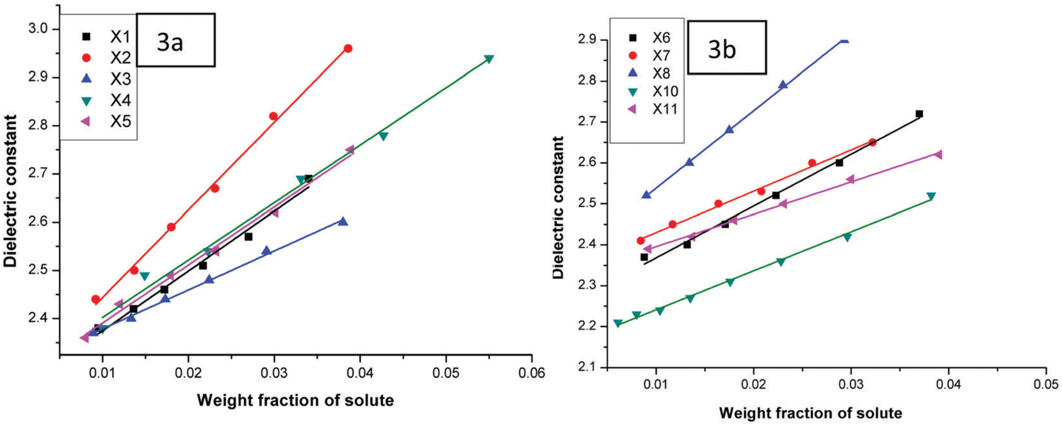

Fig. 3 Variations in dielectric constant with the weight fraction of (a) X1–X5 and (b) X6–X11.

Table 5 Energy and theoretical and experimental dipole moment values

			Dipole moment (D)		
Entry	R	Compound	Experimental	Theoretical	Energy (eV)
1	H	X1	6.25	6.00	−30416.18
2	2-OH	X2	7.83	8.45	−31485.84
3	4-OH	X3	5.22	4.72	−31485.85
4	2-OMe	X4	6.40	5.17	−33532.11
5	4-OMe	X5	6.49	6.80	−33532.12
6	4-Cl	X6	6.68	7.33	−42922.08
7	4-Br	X7	6.32	7.29	−100378.38
8	4-NO_2	X8	8.3	9.94	−35980.83
9	1-Furyl	X9	—	6.41	−30355.50
10	1-Thienyl	X10	5.59	6.53	−39144.11
11	Cinnamyl	X11	5.36	6.09	−32522.31

toluene were prepared and kept between the plates of a parallel plate capacitor. The variations of dielectric constant with the weight fraction of the solute are shown in Fig. 3a and b.

The parameter $(\partial\varepsilon/\partial\omega)$ (slope of the graph) was used to calculate the ground state dipole moment of the molecule using eqn (1), along with all other known or measured parameters and the values are given in Table 5. High dipole moment values were obtained, which indicated the unsymmetrical electronic structures, stronger intermolecular interactions and polarization of the molecules.

$$\mu_g{}^2 = \frac{3\varepsilon_0 kT}{N_A}\frac{9}{(\varepsilon^0+2)(n_0{}^2+2)}\frac{M}{\rho_0}\left(\frac{\partial\varepsilon}{\partial\omega}\right) \qquad (1)$$

In order to verify the dipole moment obtained from the experiment and to find whether the yields of the xanthene derivatives depended on the ground state energies of the molecules, the molecules were optimized using the DFT/B3LYP/6-31G* formalism and the obtained values are also presented in Table 5. The experimentally determined dipole moments for the xanthene derivatives lie in the range of 5.22–8.3 D and the theoretical values are in the range of 4.72–9.94 D. High dipole moments were observed for all the derivatives and the experimental values are in good agreement with the theoretical values. The high dipole moment values indicate the unsymmetrical electronic structures and polarization of the molecules. Attempts were made to calculate the excited state dipole moment by monitoring the solvatochromic behaviour assuming a two-level model. But the molecules did not show significant solvatochromism, so experiments for excited state dipole moment studies were not conducted. Therefore we could not calculate the change in dipole moment and thus their electrooptic properties. The optimised structures of the molecules with their corresponding dipole moment vector are given in Fig. 4.

The optimized energy (lowest possible energy of the molecule in the ground state) is depicted in Table 5. Among this, the xanthene derivative corresponding to benzaldehyde (Table 5, entry 1) showed a higher energy value (−30416.18 eV), so we expected a lower product yield compared with the others. But an excellent yield (96% yield) was observed in this case. In some

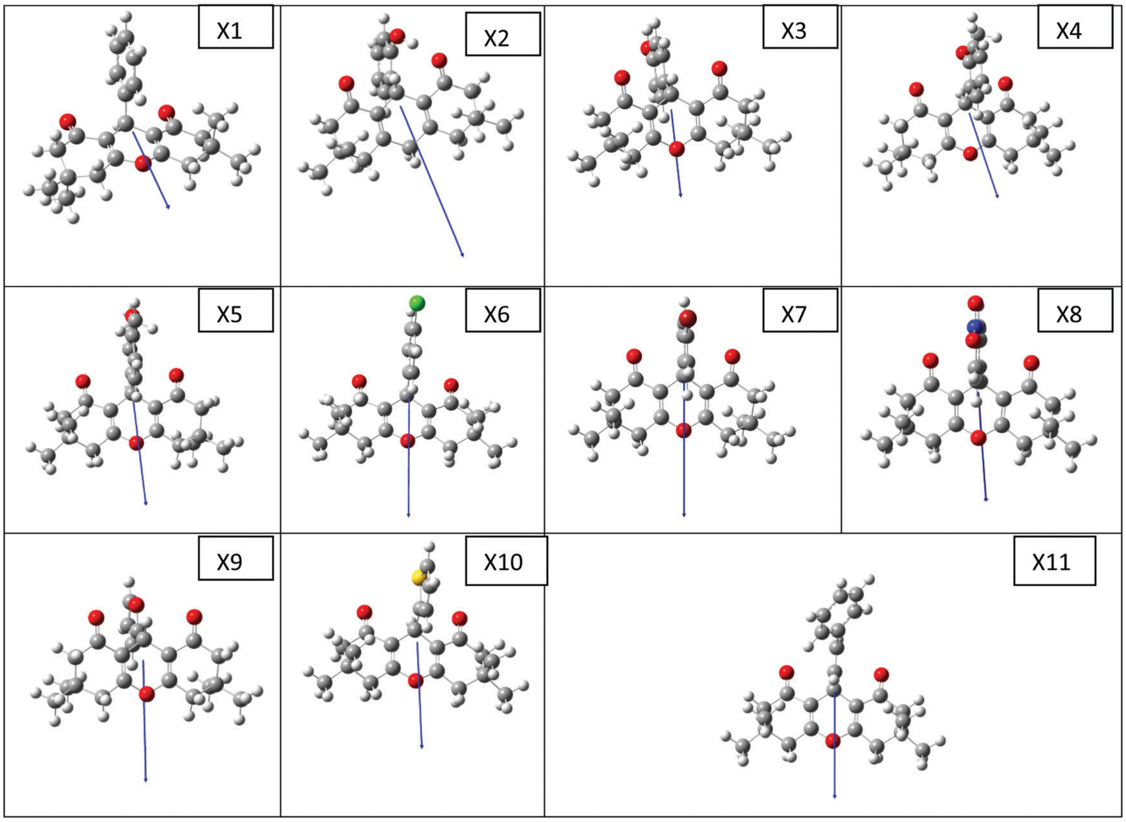

Fig. 4 Optimised structures of the synthesised 9-aryl-1,8-dioxooctahydroxanthenes with their dipole moment vectors.

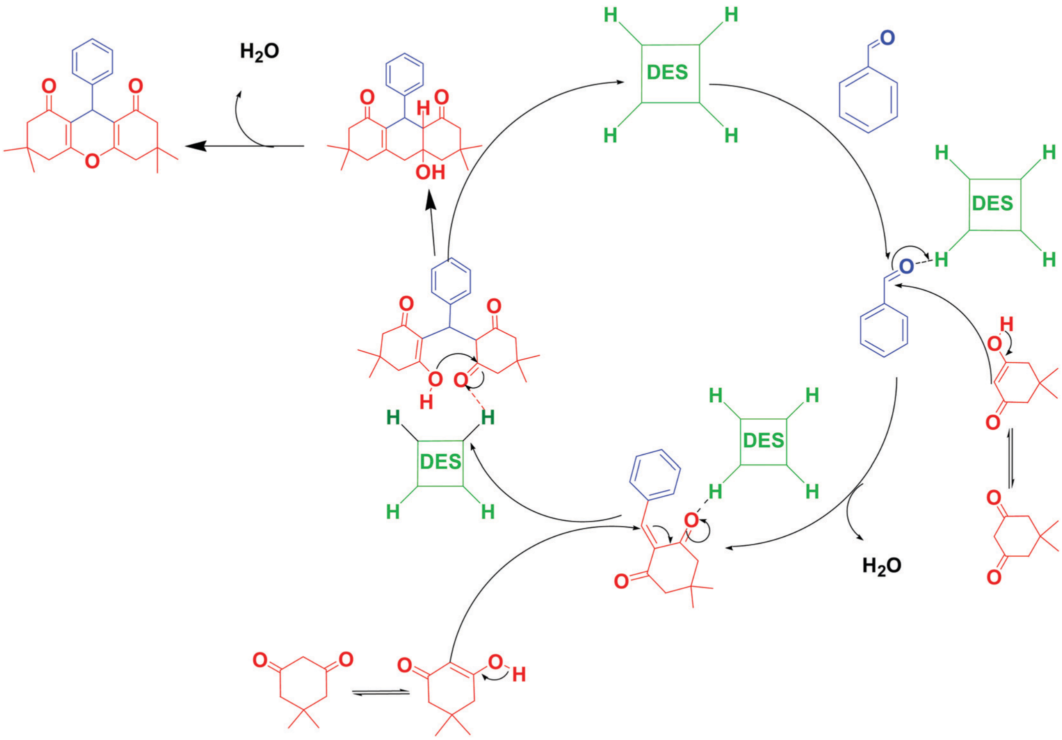

Scheme 3 Probable mechanism for the synthesis of 1,8-dioxooctahydroxanthenes in DES 2.

other derivatives, for example, for the product corresponding to cinnamaldehyde (Table 5, entry 11), lower conversion was observed due to the higher energy of the molecule compared to the others (E = −32522.31 eV) and a good agreement was observed between the theoretical and experimental results. An overall comparison led to the conclusion that the formation of xanthene derivatives was not only predicted by using optimised energy, but some additional factors (both kinetic and thermodynamic factors) must also be considered.

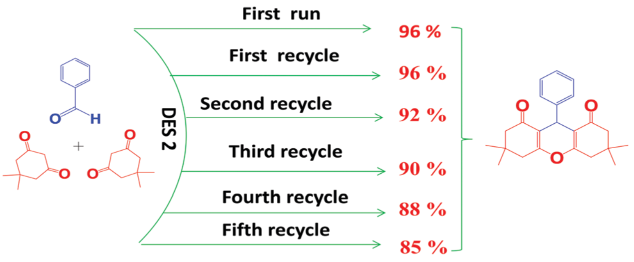

Fig. 5 Reusability of DES 2.

Probable mechanism of the reaction

A probable mechanism based on the observations is outlined in Scheme 3. First, the aldehyde was activated by the interaction of deep eutectic solvent, followed by the nucleophilic attack of dimedone to afford the Knoevenagel product. In the second step, Michael addition occurred between the active methylene of the second dimedone and the Knoevenagel condensed product. In the last step, cyclization happened with the subsequent dehydration to form 1,8-dioxooctahydroxanthenes.

Recyclability of DES 2

After completion of the reaction, the crude product was separated by adding a sufficient amount of water. The DES present in the filtrate was recovered by evaporating water under vacuum and reused for next five batches. The details of the study are given in Fig. 5.

The recovery of the catalyst was made from aqueous solution. Even after vacuum drying, some amount of water may remain with the recovered catalyst. This water may form a hydrogen bond network with the DES. This may decrease the capacity of the DES to activate the aldehyde through a H-bond activation mechanism.

Comparison with previous reports

A comparative study was also performed by selecting benzaldehyde and dimedone as model substrates for the synthesis of 9-aryl-1,8-dioxooctahydroxanthenes and the results are outlined in Table 6. Most of the recent studies are based on magnetic composites and nanoparticles (Table 6, entries 1–5) and their synthesis required multistep processes. More steps are involved in their preparation and purification. Instead of that, the DES used here can be prepared very easily by simply mixing the constituents with gentle heating and no additional purification is involved. The DES is formed with 100% atom economy and can be directly used. In addition to this, most of the reports use organic solvents, higher temperatures, and prolonged reaction times. In the present case, the DES itself can act as the catalyst and the reaction medium. By overall comparison, DES 2 provided better results in terms of easy preparation, high

Table 6 Comparison of DES 2 with some recent reports

Entry	Catalyst	Solvent	Time/temp. (°C)	Yield (%)	Reusability	Ref.
1	Sulfonamide functionalised magnetic composite	Water	40 min/100 °C	90	—	44
2	Nickel-cobalt ferrite NPs	Ethanol–water	25 min/110 °C	95	5	45
3	$CuFe_2O_4$@SiO_2@C_3-Imid-C_4SO_3-PW MNPs	—	8 min/110 °C	89	4	47
4	CoNP@SBA-15	Water	60 min/60 °C	98	10	48
5	Nickel NPs@N-doped titania nanocatalyst	Ethanol	150 min/60 °C	85	5	49
6	DES 2	—	15 min/RT	96	5	Present work

Reaction conditions: benzaldehyde (1 mmol) and dimedone (2 mmol).

yields, and dual solvent/catalyst roles and the reaction was carried out at room temperature.

Conclusion

Six deep eutectic solvents were prepared from $ZrOCl_2 \cdot 8H_2O$/$CeCl_3 \cdot 7H_2O$ with urea, ethylene glycol and glycerol and their dual activities (as catalysts and reaction media) were compared for the synthesis of 9-aryl-1,8-dioxooctahydroxanthenes at room temperature. Among the six DESs (DES 1–DES 6), excellent conversion was observed by using DES 2 (a combination of $ZrOCl_2 \cdot 8H_2O$ and ethylene glycol at a 1 : 2 ratio). The strong hydrogen bonding ability of DES 2 favoured its activity as a catalyst and its lower viscosity favoured its performance as solvent. These combined effects provided better yields of xanthene derivatives using DES 2. The applicability of DESs was checked by repeating the experiment using different aldehydes and DES 2 was reused for five batches. A comparative study was performed with some previous reports and the major advantages of the present catalyst over others included the simple preparation process of the DES without any additional purification step and its dual roles as a catalyst and a reaction medium. The photophysical properties of the synthesised xanthene derivatives were examined by UV-vis and fluorescence spectroscopy in THF. The synthesised molecules showed similar absorption maxima (around 285–295 nm) and emission maxima (around 403–404 nm) and there was no difference in the values for either electron-donating or electron-withdrawing groups. To explore the applicability of the xanthene derivatives in areas like electrooptic devices and photorefractive materials, the ground state dipole moments of all the molecules (except for the product corresponding to furfural) were calculated by the Debye–Guggenheim method using toluene as the non-polar solvent. Here, high dipole moment values were obtained, which indicated the unsymmetrical electronic structures, stronger intermolecular interactions and polarization of the molecules. But unfortunately, the molecules did not show significant solvatochromism, so experiments for excited state dipole moment studies were not conducted. The molecules were optimized using the DFT/B3LYP/6-31G* formalism. A comparison of the energies of the molecules led to the conclusion that the formation of the xanthene derivatives was not only predicted by using optimised energy, but some additional factors (both kinetic and thermodynamic factors) must also be considered to predict the reaction theoretically. A good correlation was observed between the theoretical and experimental dipole moment values for a series of substituted xanthenes.

Experimental

Preparation of deep eutectic solvents

DESs were prepared by heating the constituents (hydrogen bond donors and hydrogen bond acceptors) by gentle heating (40–60 °C) for 10–15 minutes at different molar ratios until a clear, colourless, homogeneous liquid was formed.[53–55]

Synthesis of 9-aryl-1,8-dioxooctahydroxanthenes

A mixture of aldehydes (1 mmol), dimedone (2 mmol) and DES (0.5 mmol) was stirred at RT and the progress of the reaction was monitored using TLC. After the completion of the reaction, distilled water was added and the product precipitated was filtered and analysed by TLC, GCMS, ^{1}H NMR, ^{13}C NMR and melting point measurements (ESI†).

Determination of ground state dipole moments (μ_g)

The Debye–Guggenheim method was used for the determination of the ground state dipole moments of the molecules. The static dielectric constants of the molecules (in a non-polar solvent) were measured for a series of solutions with various weight fractions of the molecules. Here toluene was used as the nonpolar solvent. The experiment was continued up to infinite dilution to calculate the dipole moment using eqn (2).

$$\mu_g{}^2 = \frac{3\varepsilon_0 kT}{N_A}\frac{9}{(\varepsilon^0+2)(n_0{}^2+2)}\frac{M}{\rho_0}\left(\frac{\partial\varepsilon}{\partial\omega}\right) \quad (2)$$

where M = molar mass of the molecule; ε_0 = permittivity of vacuum; k = Boltzmann's constant; N_A = Avogadro's constant; ε^0 = dielectric constant of the pure solvent; n_0 = refractive index of the pure solvent; ρ_0 = density of the pure solvent; ω = weight fraction; $(\partial\varepsilon/\partial\omega)$ = variation of dielectric constant with weight fraction at infinite dilution.

In this method, it was assumed that there was a negligible dependence between the refractive index of the solution of the molecule and its weight fraction.[51,57] The capacitance was measured using a HP 4277A LCZ meter operating with a frequency of 10 kHz. The capacitor used here consisted of two parallel aluminium sheets with an active area of 4.90 cm^2, which were clamped using Teflon insulators. The measurement of capacitance was carried out for different weight fractions of the solute (medium). The dielectric constant of the solution was obtained from the ratio of the capacitance of the medium to the capacitance of air. A graph was plotted between the variation of dielectric constant with the weight fraction of the solute (Fig. 3). The slope obtained from the graph is the parameter ($\partial\varepsilon/\partial\omega$), to calculate the ground state dipole moment of the molecule using eqn (2).

Conflicts of interest

There are no conflicts to declare.

Acknowledgements

The authors thank IIRBS M. G University, Kottayam, for the NMR analysis and UGC for financial support.

References

1 A. P. Abbott, G. Capper, D. L. Davies, H. L. Munro, R. K. Rasheed and V. Tambyrajah, *Chem. Commun.*, 2001, 2010–2011.
2 T. Gu, M. Zhang, J. Chen and H. Qiu, *Chem. Commun.*, 2015, **51**, 9825–9828.
3 A. Paiva, R. Craveiro, I. Aroso, M. Martins, R. L. Reis and A. R. C. Duarte, *ACS Sustainable Chem. Eng.*, 2014, **2**, 1063–1071.
4 M. B. Taysun, E. Sert and F. S. Atalay, *J. Chem. Eng. Data*, 2017, **62**, 1173–1181.
5 M. B. Taysun, E. Sert and F. S. Atalay, *J. Mol. Liq.*, 2016, **223**, 845–852.
6 J. Wang, H. Cheng, Z. Song, L. Chen, L. Deng and Z. Qi, *Ind. Eng. Chem. Res.*, 2019, **58**, 17514–17523.
7 H. Shekaari, M. T. Zafarani-Moattar and B. Mohammadi, *J. Chem. Eng. Data*, 2019, **64**, 3904–3918.
8 A. Kadyan, S. Juneja and S. Pandey, *J. Phys. Chem. B*, 2019, **123**, 7578–7587.
9 S. Filonenko, A. Voelkel and M. Antonietti, *Green Chem.*, 2019, **21**, 5256–5266.
10 L. Quirós-Montes, G. A. Carriedo, J. García-Álvarez and A. P. Soto, *Green Chem.*, 2019, **21**, 5865–5875.
11 P. Dehury, A. K. Upadhyay and T. Banerjee, *Bull. Mater. Sci.*, 2019, **42**, 1–8.
12 Y. Chen and T. Mu, *Green Energy Environ.*, 2019, **4**, 95–115.
13 T. Cai and B. H. Qiu, *Trends Anal. Chem.*, 2019, **120**, 115623–115631.
14 X. Shang, Y. Dou, Y. Zhang, J. Tan, X. Liu and Z. Zhang, *Ind. Crops Prod.*, 2019, **140**, 111724–111730.
15 Y. Dai and K. H. Row, *Molecules*, 2019, **24**, 2300–2311.
16 R. Lou, R. Ma, K. Lin, A. Ahamed and X. Zhang, *ACS Sustainable Chem. Eng.*, 2019, **7**, 10248–10256.
17 Y. Liu, H. Yan, J. Liu, W. Dong, Z. Cao, X. Hu and Z. Zhou, *Renewable Energy*, 2020, **162**, 1842–1853.
18 K. Wu, T. Su, D. Hao, W. Liao, Y. Zhao, W. Ren, C. Deng and H. Lu, *Chem. Commun.*, 2018, **54**, 9579–9582.
19 E. Sert, E. Yılmaz and F. S. Atalay, *J. Polym. Environ.*, 2019, **27**, 2956–2962.
20 B. Nian, C. Cao and Y. Liu, *ACS Sustainable Chem. Eng.*, 2019, **7**, 18174–18184.
21 T. Vo, S. D. S. Hidalgo and C. Chiang, *Dalton Trans.*, 2019, **48**, 14748–14757.
22 J. L. Liang, H. C. Cha and Y. Jahng, *Molecules*, 2011, **16**, 4861–4883.
23 J. J. Omolo, M. M. Johnson, S. F. V. Vuuren and C. B. de Koning, *Bioorg. Med. Chem. Lett.*, 2011, **21**, 7085–7088.
24 H. Marona, E. Pekala, L. Antkiewicz-Michaluk, M. Walczak and E. Szneler, *Bioorg. Med. Chem.*, 2008, **16**, 7234–7244.
25 A. G. B. Azebaze, M. Meyer, A. Valentin, E. L. Nguemfo, Z. T. Fomum and A. E. Nkengfack, *Chem. Pharm. Bull.*, 2006, **54**, 111–113.
26 E. F. Llama, C. Campo, M. Capo and M. Anadon, *Eur. J. Med. Chem.*, 1989, **24**, 391–396.
27 A. G. Banerjee, L. P. Kothapalli, P. A. Sharma, A. B. Thomas, R. K. Nanda, S. K. Shrivastava and V. V. Khatanglekar, *Arabian J. Chem.*, 2016, **9**, S480–S489.
28 K. Wang, J. Zhang, W. T. de Sousa Júnior, V. C. M. da Silva, M. C. Rodrigues, J. A. V. Morais, C. Jiang, J. P. F. Longo, R. B. Azevedo and L. A. Muehlmann, *J. Biomater. Sci., Polym. Ed.*, 2020, **31**, 1977–1993.
29 R. Kakadiya, H. Dong, A. Kumar, D. Narsinh, X. Zhang, T. Chou, T. Lee, A. Shah and T. Su, *Bioorg. Med. Chem.*, 2010, **18**, 2285–2299.
30 B. Maleki, S. Barzegar, Z. Sepehr, M. Kermanian and R. Tayebee, *J. Iran. Chem. Soc.*, 2012, **9**, 757–765.
31 H. T. Nguyen, M. Lallemand, S. Boutefnouchet, S. Michel and F. Tillequin, *J. Nat. Prod.*, 2009, **72**, 527–539.
32 C. G. Knight and T. Stephens, *Biochem. J.*, 1989, **258**, 683–689.
33 S. A. Hilderbrand and R. Weissleder, *Tetrahedron Lett.*, 2007, **48**, 4383–4385.
34 G. Pohlers and J. C. Scaiano, *Chem. Mater.*, 1997, **9**, 3222–3230.
35 M. A. Zolfigol, R. Ayazi-Nasrabadi, S. Baghery, V. Khakyzadeh and S. Azizian, *J. Mol. Catal. A: Chem.*, 2016, **418**, 54–67.
36 A. Naya, M. Ishikawa, K. Matsuda, K. Ohwaki, T. Saeki, K. Noguchi and N. Ohtake, *Bioorg. Med. Chem.*, 2003, **11**, 875–884.
37 S. Chatterjee, M. Iqbal, J. C. Kauer, J. P. Mallamo, S. Senadhi, S. Mallya, D. Bozyczko-Coyne and R. Siman, *Bioorg. Med. Chem. Lett.*, 1996, **6**, 1619–1622.
38 Y. M. Shchekotikhin and T. G. Nikolaeva, *Chem. Heterocycl. Compd.*, 2006, **42**, 28–33.
39 F. Darviche, S. Balalaie, F. Chadegani and P. Salehi, *Synth. Commun.*, 2007, **37**, 1059–1066.
40 R. Borah, P. Dutta and P. Sarma, *Curr. Chem. Lett.*, 2013, **2**, 159–166.
41 M. Seyyedhamzeh, P. Mirzaei and A. Bazgir, *Dyes Pigm.*, 2008, **76**, 836–839.
42 X. Fan, X. Hu, X. Zhang and J. Wang, *Can. J. Chem.*, 2005, **83**, 16–20.
43 D. Fang, K. Gong and Z. Liu, *Catal. Lett.*, 2009, **127**, 291–295.

44 S. Ostovar, P. Prinsen, A. Yepez, H. R. Shaterian and R. Luque, *ACS Sustainable Chem. Eng.*, 2018, **6**, 4586–4593.

45 S. Maripi, R. B. Korupolu and S. B. Madasu, *Green Sustainable Chem.*, 2017, **7**, 70–84.

46 J. Kour, M. Gupta, B. Chowhan and V. K. Gupta, *J. Iran. Chem. Soc.*, 2019, **16**, 2587–2612.

47 N. Hosseininasab, A. Davoodnia, F. Rostami-Charati, A. Khojastehnezhad and N. Tavakoli-Hoseini, *Heterocycl. Lett.*, 2018, **8**, 35–42.

48 F. Rajabi, M. P. Dios, M. Abdollahi and R. Luque, *Catal. Commun.*, 2019, **120**, 95–100.

49 Y. Rajinder, M. Gupta and J. Kour, *J. Iran. Chem. Soc.*, 2019, **16**, 1977–1992.

50 M. Salami and A. Ezabadi, *Res. Chem. Intermed.*, 2019, **45**, 3673–3686.

51 V. C. Kishore, R. Dhanya, K. Sreekumar, R. Joseph and C. S. Kartha, *Spectrochim. Acta, Part A*, 2008, **70**, 1227–1230.

52 M. J. Frisch, G. W. Trucks, H. B. Schlegel, G. E. Scuseria, M. A. Robb, J. R. Cheeseman, G. Scalmani, V. Barone, B. Mennucci, G. A. Petersson, H. Nakatsuji, M. Caricato, X. Li, H. P. Hratchian, A. F. Izmaylov, J. Bloino, G. Zheng and J. L. Sonnenberg, *et al.*, *Gaussian 09*, Gaussian, Inc., Wallingford CT, 2010.

53 M. Shaibuna, L. V. Theresa and K. Sreekumar, *Catal. Lett.*, 2018, **148**, 2359–2372.

54 M. Shaibuna, K. Hiba, L. V. Theresa and K. Sreekumar, *New J. Chem.*, 2020, **44**, 14723–14732.

55 M. Shaibuna and K. Sreekumar, *ChemistrySelect*, 2020, **5**, 13454–13460.

56 M. Shaibuna and K. Sreekumar, *Synth. Commun.*, 2021, **51**, 1742–1753.

57 C. Bosshard, G. Knopfle, P. Pretre and P. Gunter, *J. Appl. Phys.*, 1992, **71**, 1594–1605.